

Circularly Polarized 1×4 Square Slot Array Antenna by Utilizing Compacted Modified Butler Matrix and Branch Line Coupler

Saeid Karamzadeh,^{1,2} Mesut Kartal²

¹Department of Electric and Electronics Engineering, Istanbul Aydin University, Istanbul, Turkey

²Department of Electric and Electronics Engineering, Istanbul Technical University, Istanbul, Turkey

Received 19 August 2015; accepted 8 October 2015

ABSTRACT: Circularly polarized (CP), beam steering antennas are preferred to reduce the disruptive effects such as multi-path fading and co-channel interference in wireless communications systems. Nowadays, intensive studies have been carried out not only on the specific antenna array design but also their feeding networks to achieve circular polarization and beam steering characteristics. A compact broadband CP antenna array with a low loss feed network design is aimed in this work. To improve impedance and CP bandwidth, a feed network with modified Butler matrix and a compact ultra-wideband square slot antenna element are designed. With this novel design, more than 3 GHz axial ratio BW is achieved. In this study, a broadband meander line compact double box coupler with impedance bandwidth over 4.8–7 GHz frequency and the phase error less than 3° is used. Also the measured impedance bandwidth of the proposed beam steering array antenna is 60% (from 4.2 to 7.8 GHz). The minimum 3 dB axial ratio bandwidth between ports, support 4.6–6.8 GHz frequency range. The measured peak gain of the proposed array antenna is 8.9 dBic that could scan solid angle about ~ 91 degree. © 2015 Wiley Periodicals, Inc. *Int J RF and Microwave CAE* 26:146–153, 2016.

Keywords: microstrip array; square slot antenna; modified Butler matrix; coplanar waveguide feed; circularly polarized

I. INTRODUCTION

In mobile and satellite communication, some potential problems such as multipath fading and cochannel interference are the reason of using circularly polarized (CP) beam steering antennas. Actually, the main beam of the CP multiple beam antenna can be well controlled and directed to the directions subject to less interference [1]. Hitherto, many techniques to provide beamforming network such as Blass, Nolen, Butler, and other multiple input networks have been reported, but among those feed networks, Butler Matrix feed network stands out with its advantages such as being theoretically lossless, able to be implemented with a minimum number of components and beyond them, providing the circular polarization in the literature. Many different

techniques to attain CP beam steering have been presented so far [1–9]. In [2], a 2×3 CP switched microstrip antenna array was presented. In the feeding network only a single-pole multithrow microwave PIN switch was used to steer the main beam to different directions. Any directions and any number of steering beams can be realized with this structure. The main disadvantage of the reported feed network in [2] is the used line length to attain phase delay that causes a reduction in CP bandwidth. A 4×4 Butler matrix with linearly polarized elements was presented in [3]. The impedance bandwidth and 3 dB axial ratio (AR) of this antenna are 18.8% and 4.9%, respectively. In [4], a CP switched-beam patch antenna array with Butler matrix was reported.

This array has an impedance and AR bandwidth (ARBW) over a frequency range of 5.75–6.2 GHz and the main beam of the array can be scanned to any directions. A proximity-coupled L-probe feeding wideband CP antenna was exploited for wideband CP beam steering [5].

Correspondence to: Saeid Karamzadeh; e-mail: karamzadeh@itu.edu.tr

DOI: 10.1002/mmce.20947

Published online 20 October 2015 in Wiley Online Library (wileyonlinelibrary.com).

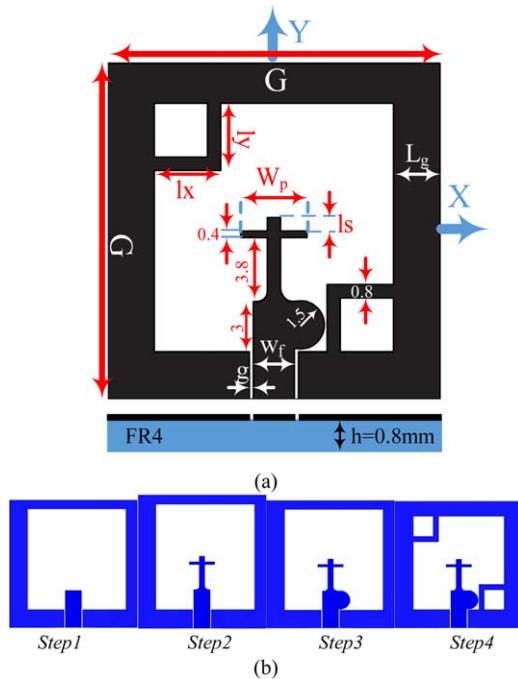


Figure 1 Configuration and design steps of the CPSSA (a) Basic structure of proposed antenna, and (b) Design steps ($G = 20$; $L_g = 1.8$; $l_x = 4$; $l_y = 4$; $L_s = 0.8$; $W_p = 4$; $g_1 = 0.6$; $g = 0.24$; $W_f = 2.48$) (all value in mm).

In the mentioned works [3–5], the use of low bandwidth microwave components such as 90° coupler, phase shifter, crossover, and single element antenna is led to decrease the impedance and the CP bandwidths. Therefore, to increase the CP beam steering bandwidth, it is preferable to use broadband components in Butler matrix feed networks. A well-known technique to improve Butler matrix feed network bandwidth is to remove the cross over structures from the network. This structure is called the modified Butler matrix [6–9], and is composed of four branch-line couplers and two 45° phase shifters without any crossovers. The purpose of this article is to design a modified broadband CP beam forming array antenna by a novel technique. To improve the impedance and CP bandwidth, following innovations have been implemented: (i) to provide broadband feed network, the use of a new modified Butler matrix including broadband double-box slow wave branch line coupler and Schiffman phase shifter helps to demand. (ii) A CP square slot antenna element which has compact size, ultrawide impedance BW and more than 3 GHz, 3 dB axial ratio BW is designed and used in the antenna array. Using coplanar waveguide (CPW) feed line and matching it with microstrip Butler feed network by two metalized via-hole are the other distinction in our design.

II. SINGLE ELEMENT

Figure 1 displays the structure and configuration of the proposed miniaturized coplanar waveguide (CPW)-fed CP

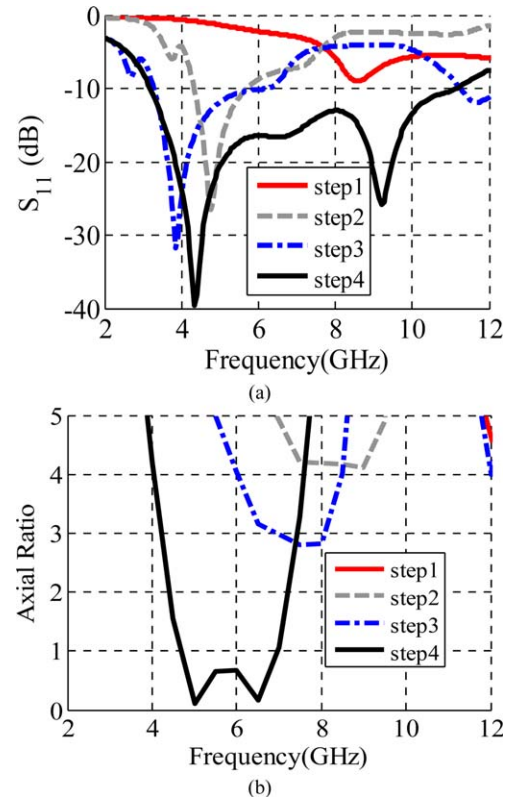


Figure 2 S_{11} and AR of antenna in four implementation steps (a) S_{11} response of antenna and (b) AR curves of antenna.

square slot antenna (CPSSA) designed in this work. The CPSSA consists of two L-shaped structure around two opposite corner of the ground line that is introduced in [10, 11], and a circular shape stub in feeding line. Following the feed line, a cross shape patch is utilized to improve the bandwidth. The proposed CPSSA is printed on a FR4 substrate with relative permittivity $\epsilon_r = 4.4$, loss $\tan \delta = 0.02$ and compact dimension of $20 \times 20 \times 0.8 \text{ mm}^3$. To achieve 50Ω input impedance, the width W_f of the CPW feedline is fixed at 2.48 mm and the feed section is separated from the ground plane by a gap of $g = 0.24 \text{ mm}$. The CP excitation of the proposed CPSSA is mainly achieved by two inverted L-shaped strips located around two opposite corners of the square slot with $l_x \times l_y$ dimensions [10, 11]. The configuration of the CPSSA was optimized using Ansoft HFSS commercial software. The stages describing the evolution of the antenna structure are shown in Figure 1b. A feed line is constructed within the rectangular slot in the first stage; in the second stage, to increase radiation resistant a cross-shape patch is embedded following the feed line; the third stage involves the feedline modification by adding a circular stub to ensure impedance matching; in final stage, two L-shape is created in two opposite of ground loop. The return loss response (S_{11}) and the 3-dB axial ratio (AR) bandwidth of the CPSSA in the four stages are displayed in Figure 2.

Results show that sequential steps improve the impedance and 3 dB AR bandwidths of the antenna. Application

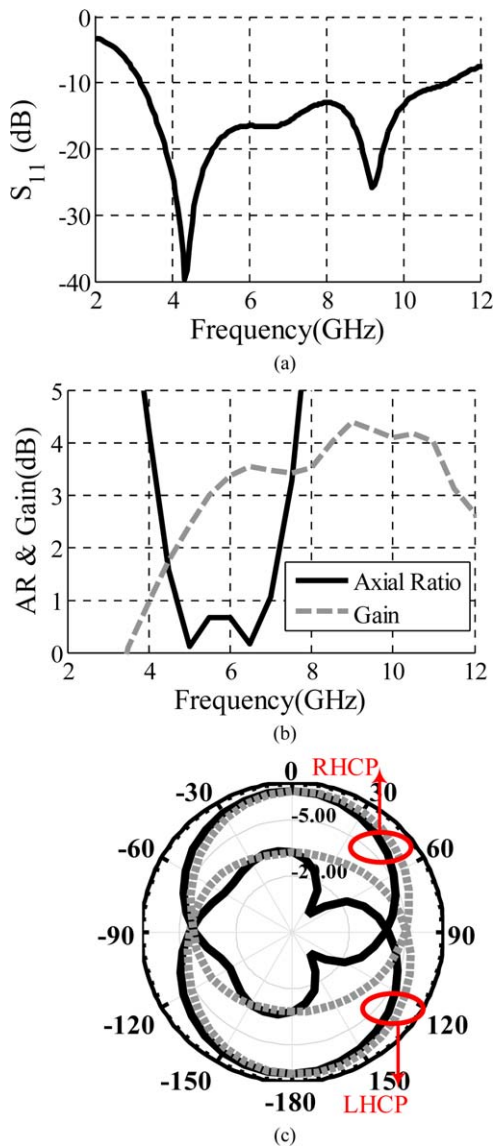


Figure 3 Simulated results of proposed single element antenna (a) return loss, (b) Gain and axial ratio, and (c) pattern at 5.5 GHz (dotted line: $\phi = 90^\circ$, straight line: $\phi = 0^\circ$).

of L-shape strip line in the fourth step creates additional surface current paths and prevents of aggregation of current in opposite corner which significantly increase impedance band width (IBW) to 8146 MHz (3097–11243

MHz) for $S_{11} \leq -10$ dB. The addition of ground-plane strip line in the fourth step significantly enhances ARBW between 4208 and 7416 GHz for an $AR \leq 3$ dB.

The simulated results of CPSSA parameters are depicted in Figure 3. Simulated return loss and simulated frequency response of the single element for AR and gain are presented in Figures 3a and [3]b, respectively. Simulated LHCP and RHCP radiation patterns of the proposed CPSS antenna for $\phi = 0^\circ$ and $\phi = 90^\circ$ is demonstrated in Figure 3c. In Figure 3c, $+z$ and $-z$ directions are RHCP and LHCP, respectively. The proposed CPSSA has an area of 400 mm^2 , which is considerably less than the previously published slot antennas as summarized in Table I. Compared to other similar types of CP slot antennas fabricated on the same substrate, the proposed antenna exhibits an impedance bandwidth which is significantly larger and with no reduction in the gain performance, as well as having a larger CP bandwidth. The gain is comparable to previous designs [1].

III. BRANCH LINE COUPLER

Figure 4 depicts the schematic of the proposed slow wave double box branch line coupler. Each section of the structure having different impedance and length consists of a meander line. The length of a unit cell of the meander line is l_i and total transverse width is W_i . The spacing between adjacent lines has the same distance and is equal to S_i . The line width of a meander line is W_{ai} . Thus, $l_i = 2 \times W_{ai} + 2 \times S_i$. The characteristic impedances of the meander line of width W_{ai} is Z_{ai} . The meander line is characterized by the characteristic impedance Z_{si} and the propagation constant β_{si} as follows [15, 16]:

$$Z_{si} = \sqrt{\frac{L_{ti}}{C_{ti}}} \quad (1)$$

$$\beta_{si} = \frac{\omega \sqrt{L_{ti} C_{ti}}}{l_i} \quad (2)$$

Where L_{ti} and C_{ti} are the total inductance and capacitance of the unit cell, respectively. Considering the high-impedance meander line in the unit cell (Z_{ai}), as shown in Figure 4b, the configuration of the meander line can be regarded as the parallel coupled lines where one end is connected, which forms a Schiffman section. For fixed

TABLE I Comparison of the Proposed CPSSA with other References.

| Ref. | Size (mm^3) | BW (GHz) | 3 dB ARBW (GHz) | Peak gain (dBic) |
|-----------|----------------------------|-----------------|-----------------|------------------|
| [10] | $70 \times 70 \times 1.60$ | 0.85 (1.75–2.6) | 0.4 (1.7–2.1) | 3.7 |
| [11] | $25 \times 25 \times 0.80$ | 1.9 (4–6.6.5) | 0.8 (4.9–5.7) | 3.6 |
| [12] | $25 \times 25 \times 0.80$ | 7.8 (3.1–10.9) | 0.7 (4.5–6.8) | 3.3 |
| [13] | $60 \times 60 \times 1.6$ | 3.65 (1.6–5.25) | 2.45 (2.4–4.85) | 3 |
| [14] | $30 \times 30 \times 9.5$ | 2.2 (5.16–7.36) | 1.4 (5.65–7.05) | 7 |
| [1] | $25 \times 25 \times 0.80$ | 7.4 (3.1–10.5) | 1.7 (4.9–6.6) | 4.5 |
| This work | $20 \times 20 \times 0.80$ | 8.1 (3.1–11.2) | 3.2 (4.2–7.4) | 4.3 |

The impedance bandwidth is for a frequency range where $VSWR \leq 2$; and ARBW is 3-dB axial-ratio bandwidth

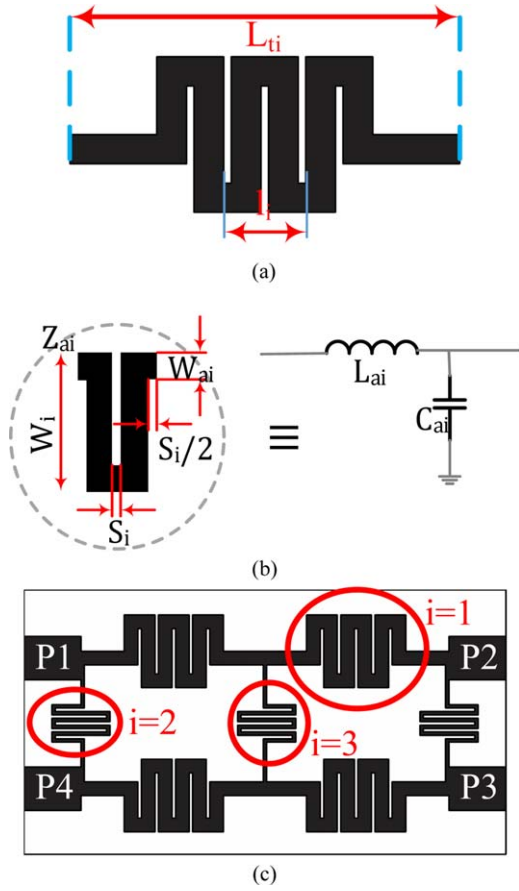


Figure 4 (a) Meander line structure, (b) unit cell and equivalent circuit unit cell, and (c) proposed 90° coupler.

W_{ai} and S_i , the image impedance Z_{li} and phase constant ϕ_i of a Schiffman section are given by [16].

$$Z_{li} = \sqrt{Z_{0ei}Z_{0oi}} \quad (3)$$

$$\cos\phi_i = \frac{\frac{Z_{0ei}}{Z_{0oi}} - \tan^2\theta_i}{\frac{Z_{0ei}}{Z_{0oi}} + \tan^2\theta_i} = \frac{1 - \left(\frac{Z_{0ei}\tan^2\theta_i}{Z_{0oi}}\right)}{1 + \left(\frac{Z_{0ei}\tan^2\theta_i}{Z_{0oi}}\right)} \quad (4)$$

Where Z_{0ei} and Z_{0oi} are the even- and odd-mode impedances of the parallel coupled lines, respectively. θ_i is the electrical length of the transmission line. In the proposed unit cell, $\theta_i = \beta_{ai} \times W_i$, where β_{ai} is the propagation constant of the microstrip line of width W_{ai} . As in the real situation $\theta_i \ll 2\pi$ and $\tan^2\theta_i \ll Z_{0ei}/Z_{0oi}$, (Eq. (4)) is further reduced to

TABLE II Length and Width of each Intersection Lettered in Figure 4 (all Values are in mm)

| | W_i | l_i | S_i | W_{ai} | L_{ti} |
|---------|-------|-------|-------|----------|----------|
| $i = 1$ | 2.56 | 1.32 | 0.12 | 0.48 | 6.28 |
| $i = 2$ | 2.04 | 0.6 | 0.12 | 0.12 | 4.12 |
| $i = 3$ | 1.82 | 0.6 | 0.12 | 0.12 | 4.12 |

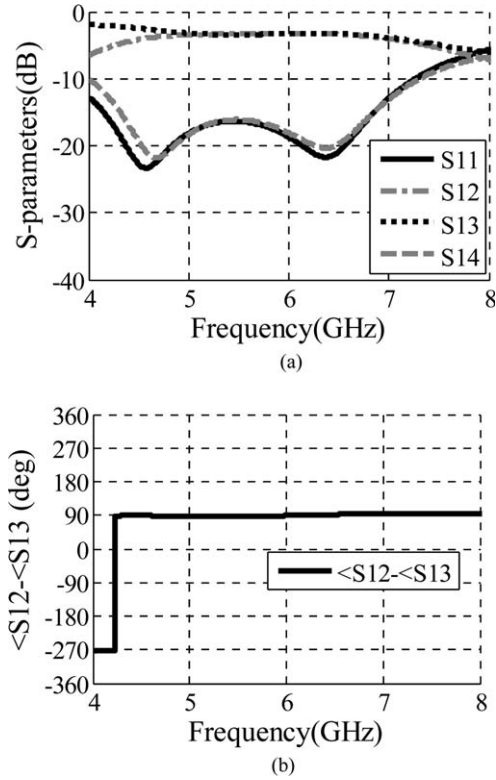


Figure 5 The simulation results of the scattering parameters of the proposed branch line coupler (a) magnitude and (b) phase.

$$\cos\phi_i \approx \left(1 - \left(\frac{Z_{0ei}\tan^2\theta_i}{Z_{0oi}}\right)\right)^2 \approx 1 - \frac{2Z_{0ei}\theta_i^2}{Z_{0oi}} \quad (5)$$

Moreover, on the basis of the Taylor-series expansion of cosine function, (Eq. (4)) can also be written as

$$\cos\phi_i \approx 1 - \frac{\phi_i^2}{2} \quad (6)$$

The propagation constant β_{fi} of a Schiffman section is

$$\beta_{fi} = \frac{\phi_i}{2W_i} \quad (7)$$

Comparing (5) and (6), it is easily seen that ϕ_i is proportional to θ_i , and consequently from (7), β_{fi} is proportional to θ_i as well as to the frequency. Consequently, the equivalent inductance and the capacitance values of the meander line in the unit cell can be calculated as follows:

$$L_{ai} = Z_{li}\beta_{fi} \times \frac{2W_i}{\omega} + Z_{ai}\beta_{ai} \times \frac{2S_i}{\omega} \quad (8)$$

$$C_{ai} = \beta_{fi} \times \frac{2W_i}{\omega Z_{li}} + \beta_{ai} \times \frac{2S_i}{\omega Z_{ai}} \quad (9)$$

The second part of the above two equations corresponds to the three short lines of length S_i in Figure 4b.

TABLE III Comparison of Published Compact Branch-Line Couplers and this Works

| Ref. | Phase error (degree) | Substrate | f_0 (GHz) | BW (GHz) | Size reduction ratio |
|-----------|----------------------|-----------|-------------|-------------|----------------------|
| [17] | >5 | FR4 | 2.4 | 0.8 (2–2.8) | 0.29 |
| [18] | ~5 | RO4003 | 5 | 2 (4–6) | 0.5 |
| [1] | ~3 | FR4 | 5.5 | 2.4 (5–7.4) | ~0.3 |
| This work | ~3 | FR4 | 5.5 | 2.2 (4.8–7) | ~0.64 |

Each conventional transmission line has been replaced by a meander line structure [1].

The length and the width of each intersection transmission line shown in Figure 4 are listed in Table II. The

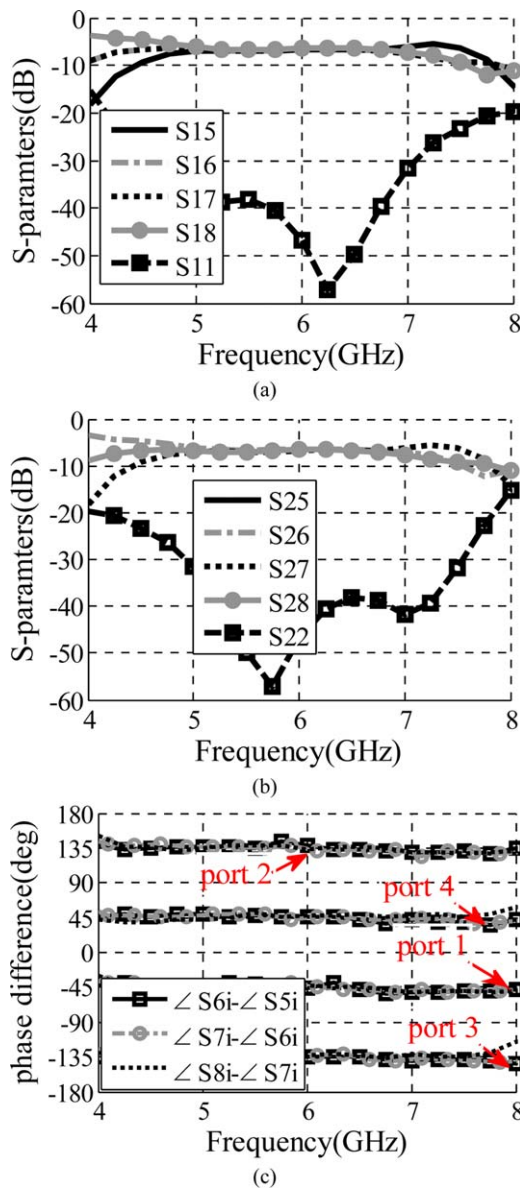


Figure 6 Magnitude results of the simulated scattering parameters of the proposed feed network for four ports. (a) Port 1, (b) Port 2, and (c) simulated phase difference for all port (i = input port).

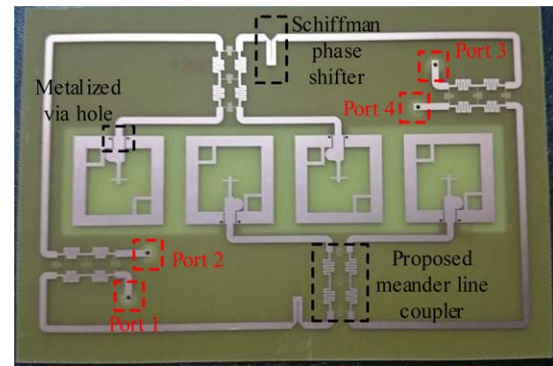


Figure 7 Photograph of the fabricated modified 4 × 4 Butler matrix with CPSS antenna elements.

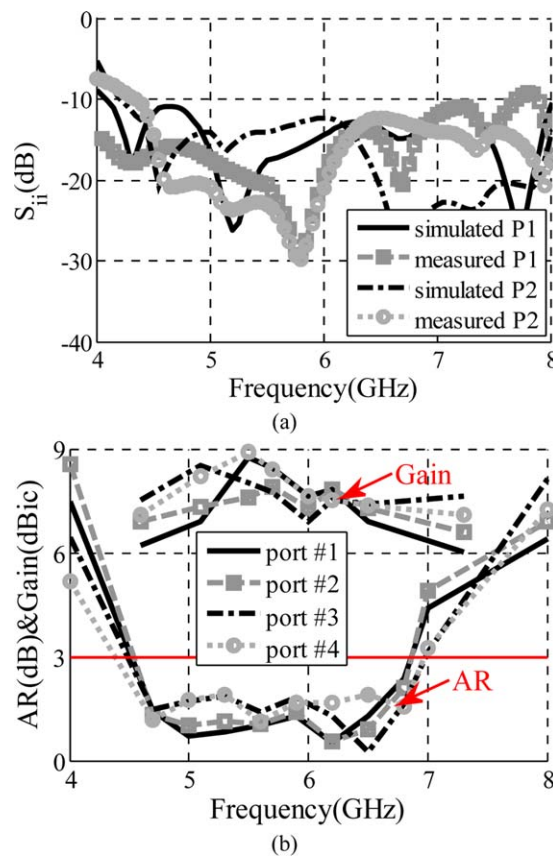


Figure 8 (a) Comparison between simulated and measured result of the return loss for ports 1 and 2 ($i = P =$ port number) and (b) the measured Gain and AR versus frequency for ports 1 to 4.

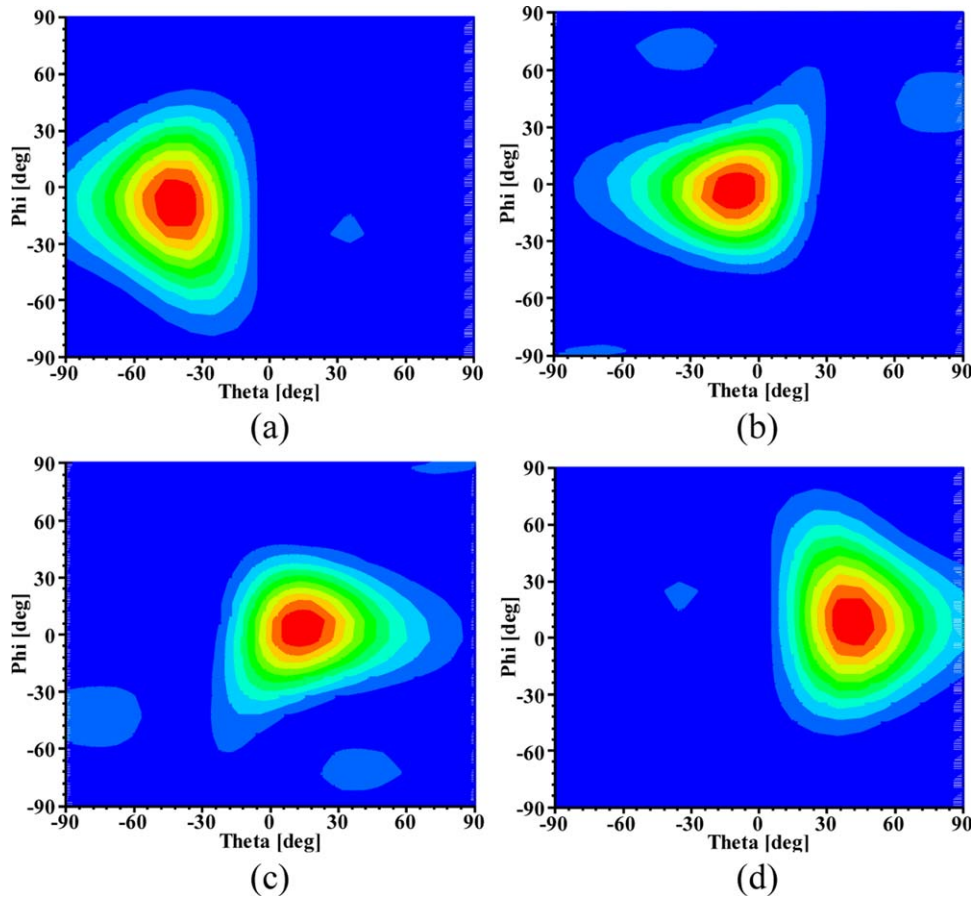


Figure 9 Simulated normalized gain patterns corresponding to ports 1–4 at 5.5 GHz. (a) port 1, (b) port 2, (c) port 3, and (d) port 4.

simulation results of the scattering parameters of the proposed branch line coupler are shown in Figure 5a and the phase division is shown in Figure 5b.

At the designed frequency, 5.5 GHz, the insertion loss is -3.4 ± 0.1 dB, the isolation is about -15 dB, and the phase difference is $90^\circ \pm 3$. Table III, summarizes the recently published branch-line hybrid couplers with reduced wavelength in transmission line and the results obtained in this work. It shows significant improvement in size reduction with wide bandwidth performance.

IV. BUTLER MATRIX FEED NETWORK

The configuration of modified Butler matrix feed network consists of two slow wave double box branch line couplers and two 45° Schiffman phase shifters, which are printed on a FR4 substrate with 0.8mm thickness and is presented in Figure 7. Proposed Butler matrix includes 4 input ports and 4 output ports and the distance between the output feeding lines is $0.46\lambda_{0-5.5\text{GHz}}$ (λ_0 -wavelength in free space).

By selecting each input (of four ports) as a driving input, the Butler matrix provides four output signals with equal amplitude and phase differences of 45° , 90° , 135° , and 180° , respectively. As a consequence, four beams with

different directions are obtained, one for each input. Proposed Butler matrix is simulated and optimized by Agilent advanced design system (ADS). Because the Butler matrix is an asymmetric feed network, therefore, just simulated results of ports 1 and 2 are presented. The simulated Magnitudes for ports 1 and 2, and simulated phase shifts for each ports are illustrated in Figures 6a and 6b. As shown in Figure 6c, the maximum magnitude and phase error for all ports are $\pm 0.35\text{dB}$ and 3° , respectively.

V. RESULT AND DISCUSSION

The designed array antenna elements are fed with the designed Butler feed network and a CP beam forming (CPBF) antenna is created. In the proposed beam steering array antenna structure, ground-loop of CPSSA is connected to ground of microstrip Butler matrix using two metalized via hole. The Proposed CPBF array antenna was fabricated (Fig. 7) and measured. Scattering parameters of CPBF array antenna was measured by Agilent 8722ES vector network analyzer. As seen in Figure 8a, there is a good agreement between the simulated and the measured return loss of the antenna, expect a frequency shifting which is a result of fabrication error.

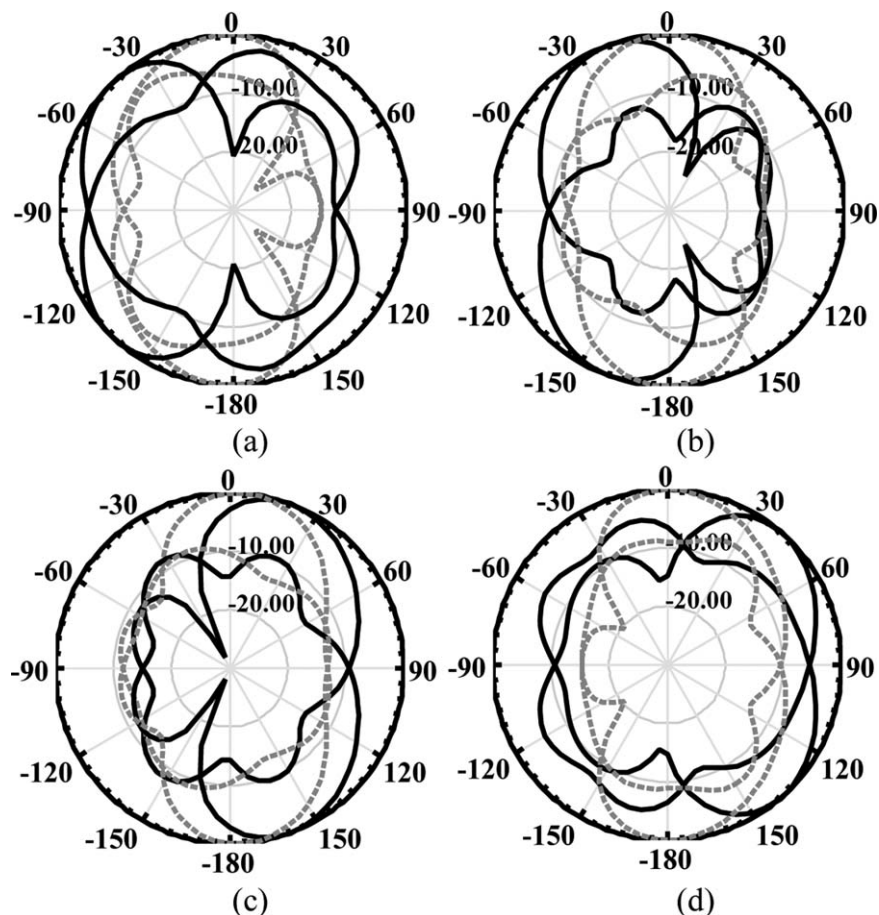


Figure 10 Measured RHCP and LHCP radiation patterns of the planar microstrip antenna array with 4×4 Butler matrix. (a) port 1, (b) port 2, (c) port 3, and (d) port 4 (dotted line: $\phi = 90^\circ$, straight line: $\phi = 0^\circ$).

From the measured results, a good impedance bandwidth over the frequency range of 4.2–7.8 GHz can be attained. The measured gain and the axial ratio versus frequency are demonstrated in Figure 8b. As seen in Figure 8b, the measured gains at 5.5 GHz for port 1, port 2, port 3, and port 4 are 8.74 dBic, 7.6 dBic, 8 dBic, and 8.9 dBic, respectively. When to use the antenna element by CPW fed the CPSSA gain, as presented in Figure 3b, is less than 4.5 dBi. By combining CPW fed with microstrip feed and matching together by metallic via, the antenna radiation resistance is increasing that is caused to enhance of radiation efficiency and Gain of single element in impedance matched range of frequency. Therefore, the antenna array can provided High gain. Same article with this condition is mentioned in [1] and [12]. In addition to, Due to changes in the phase shifting between the elements of the array, the value of angle in array factor from maximum direction in uniform angle is changing which causes to reduce of gain in beam steering antenna. To study more detail of this discussion referred to [19]. The measured AR curves are given for different feeding ports. As displayed in Figure 8b, Minimum 3dB axial ratio bandwidth is covered from 4.6 to 6.8 GHz for the worst case when excited by port 2. The calculated upper hemisphere gain patterns at

5.5 GHz are presented in Figure 9. The simulations suggest that the array provides four clearly defined beam forming states. The measured radiation patterns of 1×4 CPBF array antenna with modified 4×4 Butler matrix are displayed in Figure 10. As shown in Figures 9 and 10, the proposed antenna array has four beams at four different directions. These beams have a circular polarization diversity because a beam with RHCP will be obtained when port 1 or port 3 is selected; but if port 2 or port 4 is selected a beam with LHCP will be generated. Moreover the antenna radiated in $+z$ direction with RHCP there with radiated in $-z$ direction with LHCP. Therefore the antenna diversity in $+z$ and $-z$ direction is different, that is leads to antenna with high value of front to back ratio.

VI. CONCLUSION

A novel CP beam steering array antenna design with its compact size, good gain, and broadband AR characteristics is achieved in this work. This good performance could be obtained designing both the array antenna element with CP characteristic and the feeding network with the modified Butler matrix. The measured and the simulated results are obtained in a good agreement with the expected

performance. A significant improvement in size reduction with a wide bandwidth performance is obtained when comparing the other works in the literature.

REFERENCES

1. S. Karamzadeh, V. Rafii, M. Kartal, and B.S. Virdee, Modified circularly polarised beam steering array antenna by utilised broadband coupler and 4×4 butler matrix, *Microwaves Antennas Propag IET* 9 (2015), 975–981.
2. O. Jun, A circularly polarized switched-beam antenna array, *Antennas Wireless Propag Lett IEEE* 10 (2011), 1325–1328.
3. M. Elhefnawy and W. Ismail, A microstrip antenna array for indoor wireless dynamic environments, *IEEE Trans Antennas Propag* 57 (2009), 3998–4002.
4. C. Liu, S. Xiao, Y.-X. Guo, M.-C. Tang, Y.-Y. Bai, and B.-Z. Wang, Circularly polarized beam-steering antenna array with butler matrix network, *IEEE Antennas Wireless Propag Lett* 10 (2011), 1278–1281.
5. C. Liu, S. Xiao, Y.-X. Guo, Y.-Y. Bai, and B.-Z. Wang, Broadband circularly polarized beam-steering antenna array, *IEEE Trans Antennas Propag* 61 (2013), 1475–1479.
6. H. Hayashi, D.A. Hitko, and C.G. Sodini, Four-element planar butler matrix using half-wavelength open stubs, *IEEE Microwave Wireless Compon Lett* 12 (2002), 73–75.
7. C. Dall’Omo, T. Monediere, B. Jecko, F. Lamour, I. Wolk, and M. Elkael, Design and realization of a 4×4 microstrip Butler matrix without any crossing in millimeter waves, *Microwave Opt Technol Lett* 38 (2003), 462–465.
8. Y.J. Cheng, W. Hong, and K. Wu, Millimeter-wave multi-beam antenna based on eight-port hybrid, *IEEE Microwave Wireless Compon. Lett* 19 (2009), 212–214.
9. S. Zheng, W.S. Chan, S.H. Leung, and Q. Xue, Broad band butler matrix with flat coupling, *Electron Lett* 43 (2007), 576–577.
10. J.Y. Sze and C.C. Chang, Circularly polarized square slot antenna with a pair of inverted-L grounded strips, *IEEE Antennas Wireless Propag Lett* 7 (2008), 149–151.
11. V. Rafii, J. Nourinia, C. Ghobadi, J. Pourahmadazar, and B.S. Virdee, Broadband circularly polarized slot antenna array using sequentially rotated technique for C-band applications, *Antennas Wireless Propag Lett IEEE* 12 (2013), 128–131.
12. S. Karamzadeh, V. Rafii, M. Kartal, O.N. Ucan, and B.S. Virdee, Circularly polarised array antenna with cascade feed network for broadband application in C-band, *Electron Lett* 50 (2014), 1184–1186.
13. Nasimuddin, C. Zhi Ning, and Q. Xianming, Symmetric-aperture antenna for broadband circular polarization, *IEEE Trans Antennas Propag* 59 (2011), 3932–3936.
14. K. Agarwal and Nasimuddin, A. Alphones, Unidirectional wideband circularly polarised aperture antennas backed with artificial magnetic conductor reflectors, *Microwaves Antennas Propag IET* 7 (2013), 338–346.
15. R.E. Collin, *Foundations for microwave engineering*, 2nd ed., McGraw-Hill, New York, 1992.
16. B.M. Schiffman, “A new class of broadband microwave 90-degree phase shifters,” *IRE Trans. Microwave Theory Techn., MTT-6* (1958), 232–237. Apr.
17. S.S. Liao and J.T. Peng, Compact planar microstrip branch-line couplers using the quasi-lumped elements approach with nonsymmetrical and symmetrical t-shaped structure, *IEEE Trans Microwave Theory Techn* 54 (2006), 3508–3514.
18. C. Chen, H. Wu, and W. Wu, Design and implementation of A compact planar 4×4 microstrip butler matrix for wideband application, *Prog Electromagn Res C* 24 (2011), 43–55.
19. R.C. Hansen (2009) *Planar and circular array pattern synthesis*, in *Phased Array Antennas*, 2nd Edition, John Wiley & Sons, Inc., Hoboken, NJ, USA.

BIOGRAPHIES



Saeid Karamzadeh, received his MS degree in 2013 and he is Ph.D. candidate in Department of Communication Systems, Satellite Communication & Remote Sensing program at Istanbul Technical University now. Simultaneously, he is an instructor in the Istanbul Aydin University, Department of Electric and Electronics Engineering. His research interests include remote sensing, radar, signal processing, microwave, and Antenna design.



Mesut Kartal received his MS degree in 1993 and Ph.D. degree in 2000. Currently, he is an associate professor in the Istanbul Technical University, Department of Electronics and Communication Engineering. His research interests include remote sensing, inverse problems, RF & microwave circuit and antenna design, as well as modelling, design, simulations and analysis, and CAD techniques in high frequency region.

Mesut Kartal received his MS degree in 1993 and Ph.D. degree in 2000. Currently, he is an associate professor in the Istanbul Technical University, Department of Electronics and Communication Engineering. His research interests include remote sensing, inverse problems, RF & microwave circuit and antenna design, as well as modelling, design, simulations and analysis, and CAD techniques in high frequency region.